

t(11;19)(q21;p13) translocation in mucoepidermoid carcinoma creates a novel fusion product that disrupts a Notch signaling pathway

Giovanni Tonon^{1*}, Sanjay Modi^{1*}, Lizi Wu^{2*}, Akihito Kubo¹, Amy B. Coxon¹, Takefumi Komiya¹, Kevin O'Neil³, Kristen Stover¹, Adel El-Naggar⁴, James D. Griffin², Ilan R. Kirsch¹ & Frederic J. Kaye¹

*These authors contributed equally to this work

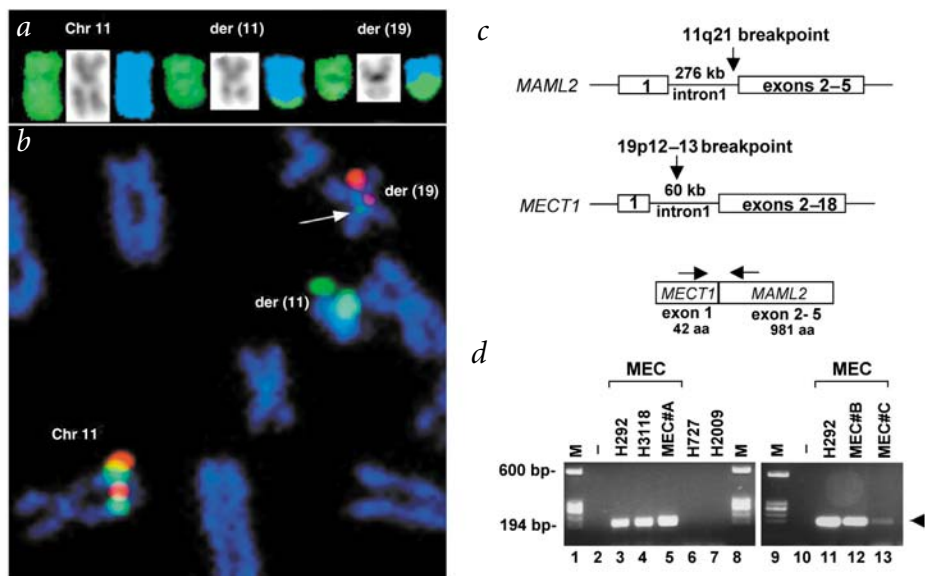
Published online 21 January 2003; doi:10.1038/ng1083

Truncation of Notch1 has been shown to cause a subtype of acute leukemia¹, and activation of Notch4 has been associated with mammary and salivary gland carcinomas of mice². Here we identify a new mechanism for disrupting Notch signaling in human tumorigenesis, characterized by altered function of a new ortholog of the *Drosophila melanogaster* Notch co-activator molecule Mastermind. We cloned the t(11;19) translocation that underlies the most common type of human malignant salivary gland tumor. This rearrangement fuses exon 1 from a novel gene of unknown function at 19p13, termed mucoepidermoid carcinoma translocated 1 (*MECT1*), with exons 2–5 of a novel member of the Mastermind-like gene family (*MAML2*) at 11q21 (ref. 3). Similar to *D. melanogaster* Mastermind and *MAML1* (refs. 4,5), full-length *MAML2* functioned as a CSL (CBF-1, suppressor of hairless and Lag-1)-dependent transcriptional

co-activator for ligand-stimulated Notch. In contrast, *MECT1*–*MAML2* activated transcription of the Notch target gene *HES1* independently of both Notch ligand and CSL binding sites. *MECT1*–*MAML2* induced foci formation in RK3E epithelial cells, confirming a biological effect for the fusion product. These data suggest a new mechanism to disrupt the function of a Notch co-activator in a common type of malignant salivary gland tumor.

Mucoepidermoid carcinoma, the most common malignant salivary gland tumor, is characterized by a t(11;19)(q14–21;p12–13) translocation, which is occasionally the sole cytogenetic alteration^{6–11}. We carried out spectral karyotyping on two mucoepidermoid carcinoma tumor cell lines, NCI-H292 and H3118, and identified a reciprocal t(11;19) translocation in both cases (Fig. 1a). Using multiple bacterial artificial

Fig. 1 t(11;19) rearrangement creates a *MECT1*–*MAML2* fusion transcript. **a**, Spectral karyotyping of mucoepidermoid carcinoma tumor cell line showing normal Chr 11 and the reciprocal t(11;19) with der(11) and der(19). The display color (left), DAPI G-banding-like (middle) and classification representation (right) are shown for each chromosome. For the classification representation, blue represents Chr 11 and green represents Chr 19. **b**, FISH analysis showing overlapping hybridization of the immediately adjacent RP11-676L3 (green) and RP11-16K5 (red) BAC clones at 11q21, and mapping of RP11-16K5 to der(19) and RP11-676L3 to der(11). Note the weak signal of the RP11-676L3 probe that maps with RP11-16K5 on der(19) (arrow). **c**, Diagram depicting the partial genomic structure of *MAML2* and *MECT1* and the approximate location of the translocation breakpoint. *MAML2* exon 1 was contained within RP11-16K5 (which mapped to der(19)). **d**, RT-PCR analysis using *MECT1* exon 1 (sense) and *MAML2* exon 2 (antisense) oligonucleotides as indicated. Size markers (M; lanes 1, 8, 9), negative control (–; lanes 2, 10) and amplified cDNA from mucoepidermoid carcinoma tumors (MEC; lanes 3–5, 11–13) and from non-mucoepidermoid carcinoma tumors (lanes 6, 7) are indicated by the arrowhead.



¹Genetics Branch, Center for Cancer Research, National Cancer Institute and the National Naval Medical Center, Bethesda, Maryland 20889, USA. ²Adult Oncology, Dana-Farber Cancer Institute and Department of Medicine, Brigham and Women's Hospital and Harvard Medical School, Boston, Massachusetts 02115, USA. ³Pulmonary Division, Department of Medicine, National Naval Medical Center, Bethesda, Maryland, USA. ⁴Department of Pathology, MD Anderson Cancer Center, Houston, Texas, USA. Correspondence should be addressed to F.J.K. (e-mail: fkaye@helix.nih.gov).

Table • 1 Focus assay in RK3E epithelial cells

| Plasmid | Number of foci ^a |
|--------------|-----------------------------|
| pFlag vector | 0 |
| MAML2 | 0 |
| MECT1-MAML2 | 31–50 |
| ICN | 58–90 |
| RAS | >100 |

Data show foci counts per 10-cm² plates scored at 3 wk using light microscopy. ^aNumber of foci is given as a range from two independent transfections, each performed in triplicate. See Web Fig. A online.

chromosome (BAC) probes for fluorescence *in situ* hybridization (FISH) analysis, we found that the adjacent clones RP11-676L3 and RP11-16K5 mapped together near band q21 on normal Chromosome 11 (Fig. 1*b*). In contrast, RP11-676L3 hybridized to the derivative Chr 11 (der(11)) and RP11-16K5 mapped to der(19) in both tumor cell lines (Fig. 1*b*). In addition, a faint signal from RP11-676L3 was detected on der(19), indicating that the breakpoint was close to the telomeric end of RP11-676L3.

Inspection of the genomic sequence in this region identified an open reading frame approximately 20 kb from the telomeric end of RP11-676L3 that was contained within an anonymous mRNA sequence (designated KIAA1819). Protein Blast search analysis showed that this gene shared similarity with *D. melanogaster Mastermind* (*mam*) and with a recently identified gene on human Chr 5, *MAML1*, that encodes a transcriptional co-activator for Notch receptors^{4,5,12,13}. Accordingly, we have designated this novel gene *MAML2*. 5' rapid amplification of cDNA ends, using RNA extracted from both mucoepidermoid carcinoma samples, identified a single amplified product using first-strand cDNA primed from the poly(A)⁺ tail or from a specific *MAML2* exon 2 sequence (data not shown). Nucleotide sequencing identified a chimeric species representing exon 1 of a novel gene at 19p12–13 (*MECT1*) fused in-frame to exons 2–5 of *MAML2* (Fig. 1*d*).

To confirm the expression of the MECT1-MAML2 chimeric product, we carried out RT-PCR using tumor RNA isolated from three primary-tumor biopsy samples from bronchopulmonary, lingual or parotid mucoepidermoid carcinomas (mucoepidermoid carcinoma A-C) and the two mucoepidermoid carcinoma

tumor cell lines (H292, parotid origin, and H3118, pulmonary origin). We detected the identical chimera in all 5 of these mucoepidermoid carcinoma samples, but not in 20 different non-mucoepidermoid carcinoma tumors (Fig. 1*d* and data not shown). Because mucoepidermoid carcinoma tumor C had a weak signal in the semi-quantitative RT-PCR, we also carried out an RNase protection assay and detected similar, steady-state levels of the *MECT1-MAML2* chimera in mucoepidermoid carcinomas B and C (data not shown). We were unable to detect the reciprocal fusion product from two different mucoepidermoid carcinoma RNA samples, which may be explained by differential promoter activity, as we detected expression of normal *MECT1* mRNA, but not of *MAML2*, in these mucoepidermoid carcinoma cell lines (data not shown).

MECT1 contains 18 exons and its predicted protein sequence has no previously defined functional motifs. In contrast, *MAML1* and *MAML2* belong to the *D. melanogaster* Mastermind-like family^{3,14}. The mammalian *MAML1* functions as a transcriptional co-activator for Notch, forming a complex in the nucleus with the intracellular domain of an activated Notch receptor (ICN) and the bifunctional transcription factor CSL⁵. Formation of the

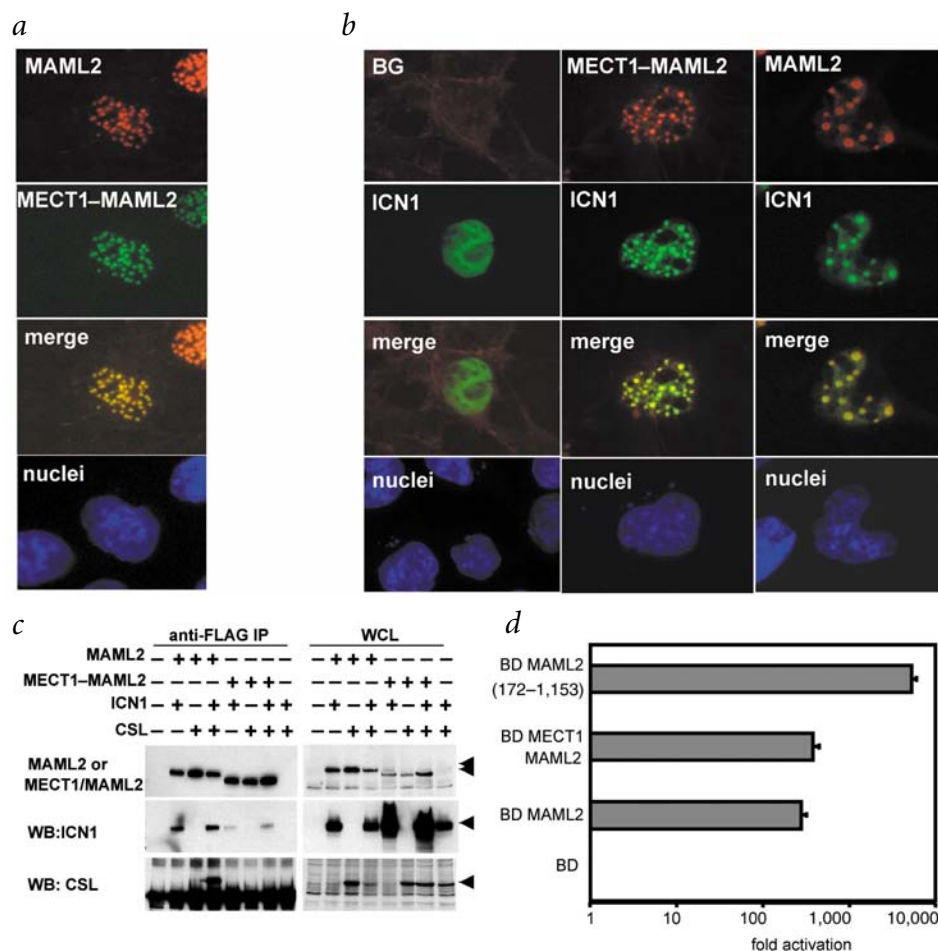
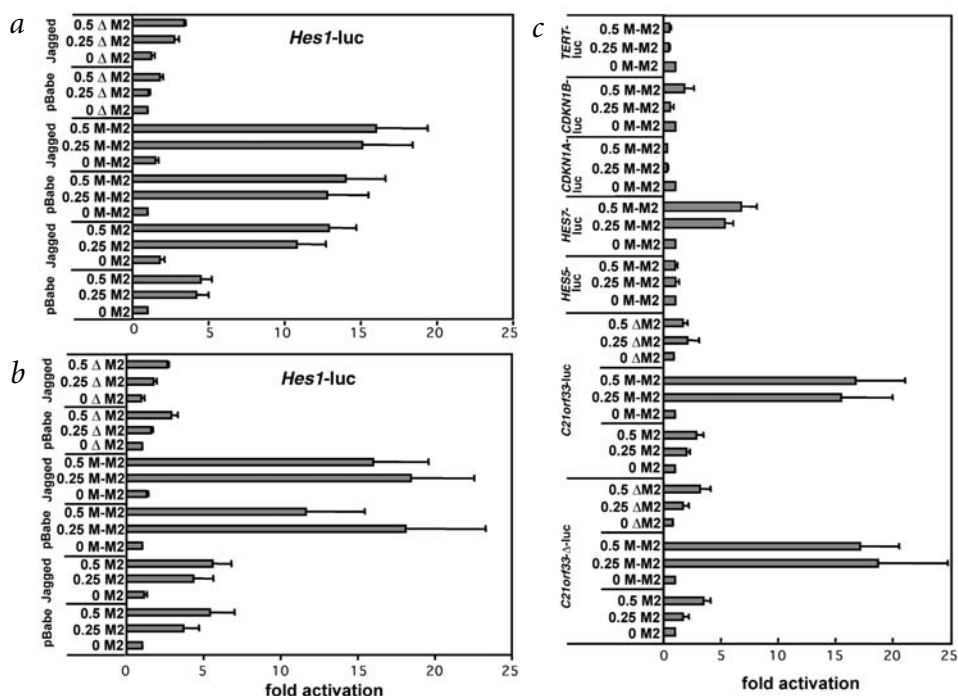


Fig. 2 MECT1-MAML2 co-localizes with ICN1, is deficient in its ability to form a ternary complex with CSL and retains a TAD. **a**, COS7 cells were transiently transfected with plasmids expressing GFP-tagged MECT1-MAML2 or Flag-tagged MAML2 proteins. Immunofluorescent staining was carried out with antibody against Flag. DAPI staining identified the nuclei (bottom panel). **b**, COS7 cells were transiently co-transfected with GFP-tagged ICN1 and empty pFlag-CMV-2 vector (BG; column 1), Flag-tagged MECT1-MAML2 (column 2) or Flag-tagged MAML2 (column 3). **c**, COS7 cells were co-transfected with different combinations of Flag-tagged MAML2, Flag-tagged MECT1-MAML2, HA-tagged ICN1 and Myc-tagged CSL as indicated. Flag-tagged immunoprecipitates (IP) or whole-cell lysates (WCL) were immunoblotted (WB) with antibodies against Flag, against HA or against Myc. **d**, U2OS cells were transfected with 0.5 μ g pG5Luc (containing four Gal4 binding sites and a firefly luciferase reporter), 25 ng pRL-TK plasmid encoding *R. reniformis* luciferase and either 0.5 μ g of Gal4 DNA binding domain (BD) only or BD fused to MECT1-MAML2, MAML2 or Δ M2. Activity was normalized to *R. reniformis* luciferase activity.

Fig. 3 MECT1–MAML2 activation is independent of Jagged2 stimulation and CSL binding sites and shows narrow promoter specificity. **a**, U2OS cells were co-transfected with 0.5 μ g of the *HES1*-luc promoter construct, 25 ng pRL-TK plasmid encoding *R. reniformis* luciferase and increasing amounts of pFlag-CMV2 plasmids (in μ g) encoding MAML2 (M2), MECT1–MAML2 (M-M2) and Δ M2. 20 h after transfection, 1×10^5 NIH 3T3 cells expressing Jagged2 or NIH 3T3 cells infected with empty pBabe virus were added to each well and luciferase activity was measured 24 h later. **b**, The same experimental design was applied with a *HES1* promoter lacking two CSL binding sites (*HES1*- Δ). **c**, U2OS cells were transfected with 0.5 μ g of the different indicated promoter reporter constructs, 25 ng pRL-TK plasmid encoding *R. reniformis* luciferase and increasing amount of MECT1–MAML2 plasmids. Luciferase reporter activity was determined as described above.



ICN–CSL–MAML1 complex activates the transcription of Notch target genes, including *HES1*, the best characterized member of the HES gene family^{4,15}.

Recently, a focus assay using epithelial cells immortalized with adenovirus E1A (RKE or RK3E cells) has been used to score the tumorigenic potential of a mutant ICN1 that was activated in the t(7;9) rearrangement of T-cell leukemia^{16,17}. Using mutant K-ras and ICN1 as positive controls, we tested the ability of pFlag–MECT1–MAML2 to generate foci using RK3E cells. Whereas vector alone and MAML2 were unable to generate foci at 3 weeks, MECT1–MAML2 induced a range of 31–50 foci per 10-cm² dish (Table 1 and Web Fig. A online). As ectopic expression of MAML2 did not induce foci formation, the biological effect of MECT1–MAML2 is probably not simply due to ectopic expression of wild-type MAML2 function.

To test the function of MECT1–MAML2 and MAML2 in Notch signaling, we compared their subcellular localization. Both proteins co-localized in a nuclear structure with a speckled staining pattern (Fig. 2a), identical to that previously described for MAML1 (ref. 5). In contrast, the peptide encoded by only exons 2–5 of MAML2 (Δ M2) localized in a diffuse, non-specific pattern (see Web Fig. B online). Co-expression of ICN1 with either MECT1–MAML2 or MAML2 induced re-localization of ICN1 from a diffuse nuclear pattern to distinct, speckled nuclear structures (Fig. 2b), as described previously for MAML1 (ref. 5). Both MECT1–MAML2 and MAML2 co-localized with ICN1 in these nuclear bodies (Fig. 2b).

We carried out immunoprecipitation experiments to determine if MECT1–MAML2 physically interacted with ICN1 (Fig. 2c). Although both MAML2 and MECT1–MAML2 co-immunoprecipitated with ICN1, MECT1–MAML2 was less effective in precipitating ICN1. This is consistent with the mapping of a Notch binding function to a conserved domain within the N-terminal region of MAML-related proteins^{5,18}, which is deleted by the MECT1–MAML2 fusion. In addition, only MAML2, and not MECT1–MAML2, co-immunoprecipitated in a ternary complex with CSL and ICN1.

A transcriptional activation domain (TAD) was previously mapped to the C-terminal region of MAML1 (ref. 5). We fused the appropriate cDNAs with the Gal4 DNA binding domain and demonstrated that MAML2 and MECT1–MAML2 encode functional TAD activity. The truncated Δ M2 also retained a high level of TAD activity (Fig. 2d).

We evaluated the ability of MECT1–MAML2 to participate in Notch signaling by examining activation of the Notch target gene *HES1*. MAML2 enhanced the Notch ligand (Jagged2)–induced activation of the *HES1* promoter, but did not enhance activation of a *HES1* promoter lacking the two endogenous CSL binding sites (*HES1*- Δ ; Fig. 3a,b). Activation of the *HES1* promoter by MECT1–MAML2, however, was independent of Notch ligand stimulation and of the CSL binding sites in the *HES1* promoter. The truncated Δ M2 did not activate *HES1* (Fig. 3a). MECT1–MAML2 showed mild activation of the *HES7* promoters in U2OS, HeLa and 293 cells, but did not activate transcription of promoters from the telomerase (*TERT*), cyclin-dependent kinase inhibitors p21 or p27 (*CDKN1A* or *CDKN1B*) or *HES5* (Fig. 3c and data not shown). In addition, we observed that MECT1–MAML2 had no effect on luciferase activity using a pGL3 SV40 promoter/enhancer vector (data not shown). These findings suggest a narrow promoter specificity for the MECT1–MAML2 product.

To confirm that MECT1–MAML2 could function in the absence of Notch ligand activation, we repeated these experiments in the presence or absence of 1 μ M of DFP-AA, a γ -secretase inhibitor that blocks cleavage and activation of the Notch receptor after ligand binding¹⁹. Co-activation of MAML2 by Jagged2 could be blocked by roughly 80% after adding the peptide inhibitor, whereas the effect on activation of MECT1–MAML2 was minimal (see Web Fig. C online).

To confirm that MECT1–MAML2 could act independently of CSL, we also tested the activation of an artificial promoter containing four copies of either a wild-type or mutant CSL binding site in front of an SV40 promoter (4 \times -wtCSL-luc and 4 \times -mtCSL-luc, respectively). Transfection of ICN1 has previously been

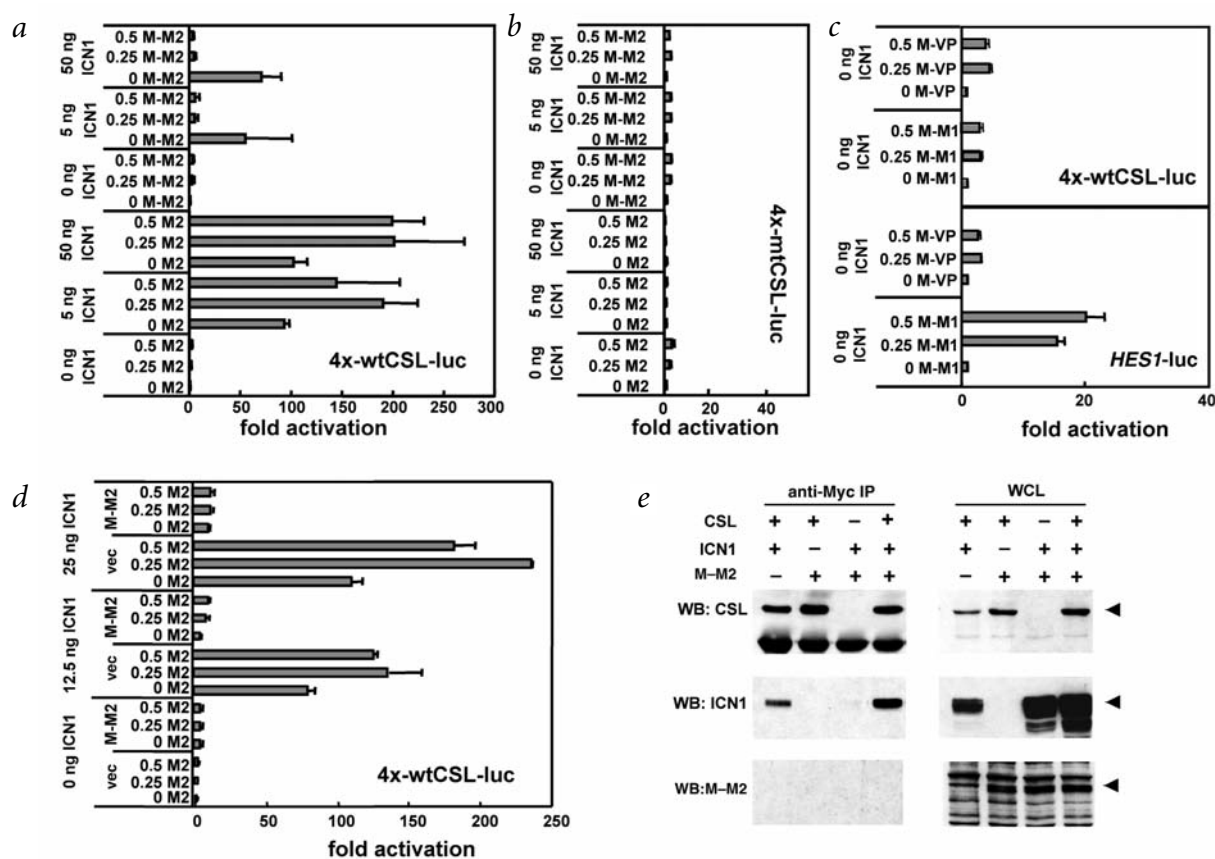


Fig. 4 Effect of MECT1–MAML2, MECT1–MAML1 and MECT1–VP16 on an artificial promoter containing four tandem CSL binding sites. Fold activation of **a**, the wild-type 4x-wtCSL-luc; **b**, mutant 4x-mtCSL-luc; or **c**, 4x-wtCSL-luc and *HES1*-luc luciferase reporter plasmids using varying amounts of co-transfected ICN1, MAML2 (M2), MECT1–MAML2 (M-M2), MECT1–MAML1 (M-M1) or MECT1–VP16 (M-VP) as indicated. **d**, No effect of MAML2 on the suppression of ICN-mediated activity by MECT1–MAML2. 0.25 μ g of MECT1–MAML2 or vector alone (vec) was co-transfected with the indicated plasmids. **e**, Co-expression of MECT1–MAML2 did not inhibit ICN or CSL binding *in vitro*. Sequential immunoprecipitation and immunoblotting was carried out as described previously for Fig. 2c except that Myc-tagged CSL was immunoprecipitated followed by immunoblotting (WB) with the indicated antibodies.

shown to activate the wild-type promoter in a CSL-dependent manner²⁰. As expected, we observed that MAML2 amplified the ICN1-induced activation of the wild-type CSL promoter but, unexpectedly, MECT1–MAML2 had an inhibitory effect. No activation was observed with the mutant CSL promoter (Fig. 4a,b). Co-transfection of increasing amounts of MAML2 could not overcome this MECT1–MAML2 inhibitory effect (Fig. 4d).

To examine the contribution of the MAML-like TAD, we replaced the MAML2 sequence with either the equivalent sequence from MAML1 (MECT1–MAML1) or an unrelated transcriptional activator, VP16 (MECT1–VP16). We observed that MECT1–MAML1, like MECT1–MAML2, could activate the *HES1* promoter independently of ICN1, whereas MECT1–VP16 had a negligible effect on the *HES1* promoter (Fig. 4c). We also observed that the chimeric MECT1–MAML1, like MECT1–MAML2, could suppress ICN1 activation of the CSL-luc promoter, whereas MECT1–VP16 had no effect (data not shown).

To test if MECT1–MAML2 interfered with ICN or CSL binding, we carried out sequential immunoprecipitation and immunoblotting of CSL from cells cotransfected with the indicated plasmids (Fig. 4e). We again confirmed that MECT1–MAML2 was not detectable in the immunoprecipitates with antibodies against CSL, and we observed that ectopic expression of MECT1–MAML2 did not seem to inhibit ICN binding to CSL *in vitro* (Fig. 4e). Therefore, although the mecha-

nism for MECT1–MAML2 function is still undefined, these data suggest that the fusion product may compete with other essential components of the transcriptional machinery^{21,22}.

Consistent with the activation effect of MECT1–MAML2 on the *HES1* promoter *in vitro*, we detected high levels of expression of *HES1* mRNA in the parotid and lung mucoepidermoid carcinoma lines H292 and H3118 relative to the levels of *HES1* expression observed in non-mucoepidermoid carcinoma lung cancer lines or in the immortalized HSY parotid duct cells using both RT–PCR and a more quantitative RNase protection assay. In addition, transient transfection of the cDNA encoding the MECT1–MAML2 fusion into normal HSY cells induced *HES1* mRNA at 48 h relative to mock-transfected HSY cells (Fig. 5).

Whereas specific chromosomal rearrangements are commonly observed in hematopoietic and mesenchymal stromal tumors, <1% of all epithelial carcinomas show a recurrent, pathogenic chromosomal alteration¹¹. Mucoepidermoid carcinoma, therefore, represents a new epithelial tumor model system in which a chimeric gene product may disrupt Notch signaling by a new mechanism. Defining the mechanism underlying the activation of *HES1* by MECT1–MAML2 and the potential contribution from MECT1 will provide further insights into Notch signaling in both normal cells and tumors carrying the t(11;19) translocation. Ultimately, MECT1–MAML2 may represent a useful target for the development and testing of novel molecular diagnostic and therapeutic strategies.

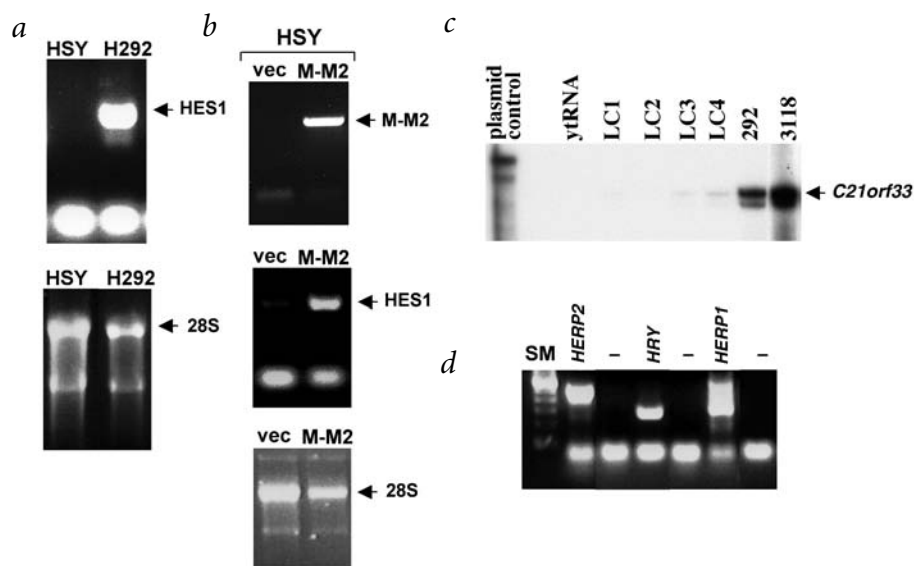


Fig. 5 Induction of Notch target genes by the MECT1-MAML2 product *in vivo*. **a**, RT-PCR using total RNA extracted from immortalized, parotid ductal cells (HSY) or the tumor line H292. **b**, Transient transfection of vector alone (vec) or MECT1-MAML2 (M-M2) into HSY cells. The 28S ribosomal signals from the RNA samples used is indicated. **c**, RNase protection assay using 10 μ g of total RNA from indicated tumor samples: yeast tRNA negative control (ytRNA), non-mucoepidermoid carcinoma lung cancer lines (LC1-4) and mucoepidermoid carcinoma samples (292, 3118). *HES1*-specific signal is indicated by the arrow. The positive control DNA plasmid signal migrates slightly more slowly owing to the inclusion of non-*HES1* plasmid polylinker cloning sites within the antisense α^{32} P[UTP] *HES1* RNA probe. **d**, Agarose gel electrophoresis showing expression of the indicated Notch target genes by RT-PCR in H292 cells. -, negative template control lanes. SM, size markers.

Methods

Tumor samples. Tumor cell lines and primary mucoepidermoid carcinoma samples were obtained from the National Naval Medical Center and MD Anderson Cancer Center following institutionally approved tissue procurement protocols. We cultured human U2OS osteosarcoma cells in Dulbecco's modified Eagle's medium (DMEM) containing 10% Fetalclone I serum (HyClone Laboratories), COS7 cells in RPMI 1640 medium supplemented with 10% fetal calf serum (FCS) and HeLa cells and 293 cells in DMEM with 10% FCS. We maintained NIH 3T3 cells transduced by pBABE retrovirus encoding Jagged2 or empty pBABE retrovirus in DMEM containing 10% FCS and 1 mg ml⁻¹ of puromycin.

Spectral karyotyping. The spectral karyotyping hybridization protocol has been described in detail elsewhere²³. We obtained specific chromosomes by high-resolution flow sorting, and then amplified them by two consecutive rounds of degenerate oligo-primed-PCR amplification. We used Spectrum Orange (Vysis), rhodamine 110 (Perkin Elmer) and Texas Red (Molecular Probes) for direct labeling and used biotin-16-dUTP and digoxigenin-11-dUTP (Roche) for indirect labeling. After hybridization, we detected biotin with Avidin-Cy5 (Amersham) and digoxigenin-11-dUTP with mouse antibody against digoxin (Sigma) followed by sheep antibodies against mouse custom-conjugated to Cy5.5 (Amersham). We counterstained the slides with 4,6-diamidino-2-phenylindole (DAPI; Sigma) and covered them with antifade solution (Vector). We acquired spectral images with an SD200 SpectraCube system (Applied Spectral Imaging) mounted on a Leica DMRBE microscope (Leica) through a custom-designed triple bandpass optical filter (SKY v.3; Chroma Technology). We carried out spectrum-based classification of the raw spectral images using SKYView 1.6 software (Applied Spectral Imaging).

Fluorescence *in situ* hybridization (FISH) analysis. BAC clones were purchased from Research Genetics or Oakland BAC/PAC Resources or were provided by R. Jonescu (RP11-16K5). For the FISH analysis, we labeled BAC clones by nick translation. We acquired images using a Sensys CCD camera (Photometrics) and Q-FISH software (Leica Microsystems Imaging Solutions).

Nucleic acid analyses. We obtained total RNA from tumor samples using guanidine isothiocyanate methodology and subjected it to 5' and 3' RACE using conditions recommended by the manufacturer (SmartRace, Clontech). We carried out RT-PCR with gene-specific oligonucleotides as recommended by the manufacturer (Amersham Pharmacia Biotech). We subcloned the cDNAs encoding MAML2, MECT1-MAML2 and truncated Δ M2 (amino acids 172-1,153) into a CMV-2-driven expression vector in-frame with the sequence encoding the Flag tag (pFlag-CMV2) and into the pEGFP-C3 (Clontech) and pBIND (Promega) vectors. We confirmed all

constructs by nucleotide sequencing and immunoblotting. The full-length *MECT1-MAML2* was cloned as a *Sall*-*NotI* fragment into pEGFP-C3 and pBIND. We used hemagglutinin (HA)-tagged ICN1 and Myc-tagged CSL, which have been previously described⁵. *HES1*-luc contains the -194 to +160 promoter fragment of *HES1* cloned upstream of the firefly luciferase gene in the pGL2-basic vector¹³. *HES1*- Δ -luc, derived from *HES1*-luc, has a deletion removing the two CSL binding sites¹³. *TERT*-luc was obtained by cloning 2.5 kb of the hTERT promoter²⁴ into pGL3-basic vector. *CDKN1A*-luc²⁵, *CDKN1B*-luc²⁶, *HES5*-luc²⁷ and *HES7*-luc²⁸ have been previously described. pRL-TK (Promega) encodes *Renilla reniformis* luciferase under the control of thymidine kinase promoter and was used to normalize firefly luciferase activities for transfection efficiency. pSG5-luc (Promega) is a firefly luciferase reporter plasmid that contains five copies of Gal4 binding site upstream of a minimal TATA box. We carried out RNase protection assays by overnight hybridization of 10 μ g total RNA from the indicated tumor samples with an antisense *HES1* RNA probe followed by digestion with RNase A and denaturing gel electrophoresis as previously described²⁹.

Protein studies. We purchased mouse antibody against Flag (clone M2, Sigma), mouse antibody against HA (clone HA.11, Babco), mouse antibody against Myc (clone 9E10, Clontech) and horseradish peroxidase-coupled goat antibody against mouse (Amersham). We carried out transfections using Superfect transfection reagent (QIAGEN) according to the manufacturer's instructions. 48 h after transfection, we washed cells with ice-cold phosphate-buffered saline and lysed them *in situ* with a solution containing 20 mM Tris (pH 8.0), 150 mM NaCl, 1% Nonidet P-40 (w/v), 10% glycerol (w/v), 100 mM NaF, 1 mM phenylmethylsulfonyl fluoride, 20 mg ml⁻¹ aprotinin, 1 mM sodium orthovanadate and 40 mg ml⁻¹ leupeptin. After incubation on ice for 30 min, we centrifuged cell lysates at 12,000g for 15 min at 4 °C. We incubated cleared lysates with antibody against Flag (M2 at 1:500) and antibody against mouse IgG agarose (Sigma) for 4 h or overnight at 4 °C. We then subjected the washed pellets to SDS-PAGE and western blotting using antibodies as indicated. We incubated washed membranes with horseradish peroxidase-coupled secondary antibodies for 1 h, washed them again and stained them using a chemiluminescent method (ECL; Amersham).

Luciferase assays. We seeded 1 \times 10⁵ cells per well for U2OS cells and HeLa cells or 2 \times 10⁵ cells per well for 293 cells onto six-well plates 1 d before transient co-transfection with combinations of expression plasmid DNA as indicated. We kept the total amounts of plasmids constant by adding appropriate amounts of empty vectors without inserts. We collected transfected cells 48 h after transfection and measured luciferase activities in a Berthold luminometer (Lumat LB9507) using the dual luciferase reporter assay system (Promega). We added DFP-AA to the cell culture medium at

1 μ M in dimethylsulfoxide and changed the medium daily. Control cells were treated with dimethylsulfoxide alone. We normalized the relative luciferase activities to *R. reniformis* luciferase activity.

RK3E assay. We obtained RK3E cells from American Type Culture Collection³⁰ and propagated them in DMEM supplemented with 10% FCS and antibiotics as recommended. We transfected 5×10^5 cells with 4 μ g of the indicated plasmids using lipofectamine reagent (Clontech). We fixed plates in 10% methanol/10% acetic acid, stained them with 0.1% crystal violet in ethanol and scored them for foci at 3 wk.

GenBank accession numbers. *MAML2*, AY040322; *MECT1*, AY040323; MECT1–MAML2 peptide, AY040324.

Note: Supplementary information is available on the Nature Genetics website.

Acknowledgments

We are grateful to M. Kuehl, P. Aplan and T. Ried for helpful suggestions; P. Gao and J. Liu for their help; B. Baum for providing the HSY cells; M. Wolfe for providing the γ -secretase inhibitor; and A. Capobianco for advice on the RK3E assay. We acknowledge partial support by an American Society of Hematology Scholar Award and a General Motors Cancer Research Scholar Award (L.W.).

Competing interests statement

The authors declare competing financial interests: see the Nature Genetics website (<http://www.nature.com/naturegenetics>) for details.

Received 24 September; accepted 20 December 2002.

- Ellisen, L.W. *et al.* *TAN-1*, the human homolog of the *Drosophila notch* gene, is broken by chromosomal translocations in T lymphoblastic neoplasms. *Cell* **66**, 649–661 (1991).
- Jhappan, C. *et al.* Expression of an activated Notch-related *int-3* transgene interferes with cell differentiation and induces neoplastic transformation in mammary and salivary glands. *Genes Dev.* **6**, 345–355 (1992).
- Wu, L., Sun, T., Kobayashi, K., Gao, P. & Griffin, J.D. Identification of a family of mastermind-like transcriptional coactivators for mammalian notch receptors. *Mol. Cell. Biol.* **22**, 7688–7700 (2002).
- Artavanis-Tsakonas, S., Matsuno, K. & Fortini, M.E. Notch signaling. *Science* **268**, 225–232 (1995).
- Wu, L. *et al.* *MAML1*, a human homologue of *Drosophila mastermind*, is a transcriptional co-activator for NOTCH receptors. *Nat. Genet.* **26**, 484–489 (2000).
- Johansson, M. *et al.* Translocation 11;19 in a mucoepidermoid tumor of the lung. *Cancer Genet. Cytogenet.* **80**, 85–86 (1995).
- Horsman, D.E., Berean, K. & Durham, J.S. Translocation (11;19)(q21;p13.1) in mucoepidermoid carcinoma of salivary gland. *Cancer Genet. Cytogenet.* **80**, 165–166 (1995).
- El-Naggar, A.K., Lovell, M., Killary, A.M., Clayman, G.L. & Batsakis, J.G. A mucoepidermoid carcinoma of minor salivary gland with t(11;19)(q21;p13.1) as the only karyotypic abnormality. *Cancer Genet. Cytogenet.* **87**, 29–33 (1996).
- Dahlenfors, R., Wedell, B., Rundrantz, H. & Mark, J. Translocation(11;19)(q14-21;p12) in a parotid mucoepidermoid carcinoma of a child. *Cancer Genet. Cytogenet.* **79**, 188 (1995).
- Dahlenfors, R., Lindahl, L. & Mark, J. A fourth minor salivary gland mucoepidermoid carcinoma with 11q14-21 and 19p12 rearrangements. *Hereditas* **120**, 287–288 (1994).
- Mitelman, F. Recurrent chromosome aberrations in cancer. *Mutat. Res.* **462**, 247–253 (2000).
- Xu, T., Rebay, L., Fleming, R.J., Scottgale, T.N. & Artavanis-Tsakonas, S. The Notch locus and the genetic circuitry involved in early *Drosophila* neurogenesis. *Genes Dev.* **4**, 464–475 (1990).
- Jarriault, S. *et al.* Signalling downstream of activated mammalian Notch. *Nature* **377**, 355–358 (1995).
- Petcherski, A.G. & Kimble, J. Mastermind is a putative activator for Notch. *Curr. Biol.* **10**, R471–R473 (2000).
- Kojika, S. & Griffin, J.D. Notch receptors and hematopoiesis. *Exp. Hematol.* **29**, 1041–1052 (2001).
- Dumont, E. *et al.* Neoplastic transformation by Notch is independent of transcriptional activation by RBP-J signalling. *Oncogene* **19**, 556–561 (2000).
- Capobianco, A.J., Zagouras, P., Blaumueller, C.M., Artavanis-Tsakonas, S. & Bishop, J.M. Neoplastic transformation by truncated alleles of human *NOTCH1/TAN1* and *NOTCH2*. *Mol. Cell. Biol.* **17**, 6265–6273 (1997).
- Petcherski, A.G. & Kimble, J. LAG-3 is a putative transcriptional activator in the *C. elegans* Notch pathway. *Nature* **405**, 364–368 (2000).
- Wolfe, M.S. γ -Secretase inhibitors as molecular probes of presenilin function. *J. Mol. Neurosci.* **17**, 199–204 (2001).
- Hsieh, J.J. *et al.* Truncated mammalian Notch1 activates CBF1/RBPJk-repressed genes by a mechanism resembling that of Epstein-Barr virus EBNA2. *Mol. Cell. Biol.* **16**, 952–959 (1996).
- Wallberg, A.E., Pedersen, K., Lendahl, U. & Roeder, R.G. p300 and PCAF act cooperatively to mediate transcriptional activation from chromatin templates by Notch intracellular domains *in vitro*. *Mol. Cell. Biol.* **22**, 7812–7819 (2002).
- Fryer, C.J., Lamar, E., Turbachova, I., Kintner, C. & Jones, K.A. Mastermind mediates chromatin-specific transcription and turnover of the Notch enhancer complex. *Genes Dev.* **16**, 1397–1411 (2002).
- Tonon, G. *et al.* Spectral karyotyping combined with locus-specific FISH simultaneously defines genes and chromosomes involved in chromosomal translocations. *Genes Chromosom. Cancer* **27**, 418–423 (2000).
- Greenberg, R.A. *et al.* Telomerase reverse transcriptase gene is a direct target of c-Myc but is not functionally equivalent in cellular transformation. *Oncogene* **18**, 1219–1226 (1999).
- Tang, H.Y. *et al.* Constitutive expression of the cyclin-dependent kinase inhibitor p21 is transcriptionally regulated by the tumor-suppressor protein p53. *J. Biol. Chem.* **273**, 29156–29163 (1998).
- Kwon, T.K., Nagel, J.E., Buchholz, M.A. & Nordin, A.A. Characterization of the murine cyclin-dependent kinase inhibitor gene p27Kip1. *Gene* **180**, 113–120 (1996).
- Beatus, P., Lundkvist, J., Oberg, C. & Lendahl, U. The notch 3 intracellular domain represses notch 1-mediated activation through *Hairy/Enhancer of split* (HES) promoters. *Development* **126**, 3925–3935 (1999).
- Besho, Y., Miyoshi, G., Sakata, R. & Kageyama, R. *Hes7*: a bHLH-type repressor gene regulated by Notch and expressed in the presomitic mesoderm. *Genes Cells* **6**, 175–185 (2001).
- Winter, E., Yamamoto, F., Almoguera, C. & Perucho, M. A method to detect and characterize point mutations in transcribed genes: amplification and overexpression of the mutant *c-Ki-ras* allele in human tumor cells. *Proc. Natl. Acad. Sci. USA* **82**, 7575–7579 (1985).
- Ruppert, J.M., Vogelstein, B. & Kinzler, K.W. The zinc-finger protein GLI transforms primary cells in cooperation with adenovirus E1A. *Mol. Cell. Biol.* **11**, 1724–1728 (1991).

t(11;19)(q21;p13) translocation in mucoepidermoid carcinoma creates a novel fusion product that disrupts a Notch signaling pathway

G Tonon, S Modi, L Wu, A Kubo, AB Coxon, T Komiya, K O'Neil, K Stover, A El-Naggar, J D Griffin, I R Kirsch & F J Kaye

Nat. Genet. **33**, 208–213 (2003).

After the authors returned corrected proofs, some changes to Figure 5 were mistakenly omitted from the final version. In Figure 5c, *C21orf33* should read *HES1* and in Figure 5d *HRY* should read *HES1*. A corrected version of Figure 5 appears below.

